Multi-Axis Planinng of a Hybrid Material Deposition and Removal Combined Process

Jun Zhang[1], Frank Liou[*2]

[1]Autodesk Inc., Novi, MI 48375

[2]Department of Mechanical and Aerospace Engineering, Missouri University of Science and Technology, Rolla, MO 65409-0050

[*]liou@mst.edu

Abstract- **In a blown powder metal deposition process, a multi-axis hybrid manufacturing system, including a material deposition and a material removal system with more than 3-aixs mobility, is highly desirable in the building complex parts. However, the multi-axis planning process is quite complex. In order to address this issue, a parametric representation of STL-based layer geometry is presented in this paper for a multi-axis material deposition and removal process to build a fully functional part without support structures. This multi-axis process can build 3-D layers in which layer thickness is not uniform. By utilizing the advantage of five-axis motion to build non-uniform 3-D layers, the ability to deposit material without support structures is increased. However, in some cases, the deposition process cannot produce the desired geometry of a 3-D layer, and thus the machining process is needed. The algorithms presented in this paper reconstruct the parametric curve from the STL format for the machining process to achieve the desired accuracy by interpolating more points between given points.**

Keywords- Process planning; Additive Manufacturing; Hybrid

I. INTRODUCTION

Manufacturers always look for ways to satisfy customer needs by providing products in the shortest time and at the lowest cost with best quality. Rapid prototyping (RP), a manufacturing process started in mid 80s, gives industry an approach to achieve that goal. The process quickly produces a part by depositing material layer by layer. The materials of most commercial systems are polymers, which result in an intermediate step between CAD models and final products. Recently some focus of researches has been on metal direct deposition systems to obtain fully functional parts. Traditional Additive Manufacturing (AM) processes that only include the material additive process sometimes cannot achieve the desired accuracy and surface finish, which are attributed to the difficulty of controlling the geometry in the material addition such as metal deposition. As shown in Fig. 1, a combination of the deposition process and the machining process is a solution to this problem. However, this introduces new problems in terms of data representation of the layers. Currently, the STL format is an industrial standard for AM systems. The layers generated from the slicing process consist of many segments. Most of the surface cutting algorithms are based on the parametric representation of the surface. Therefore, the reconstruction of curves and surfaces from discrete points is required for the hybrid processes.

(a) Deposition process to form net shape

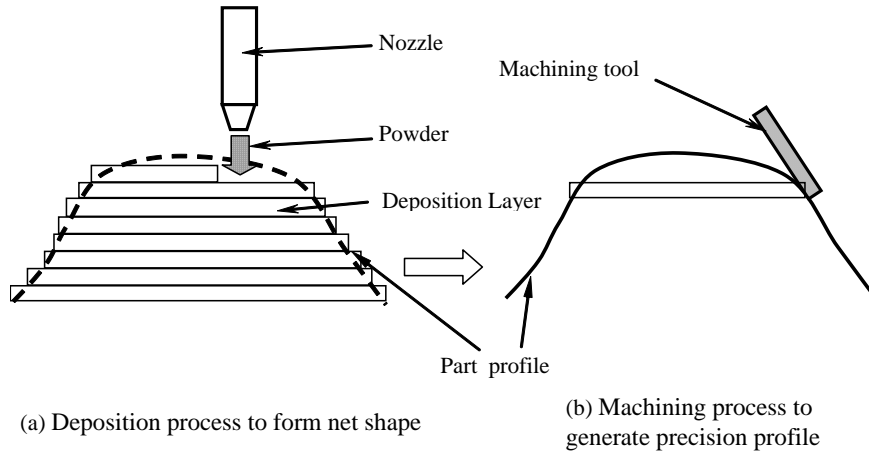(b) Machining process to generate precision profile
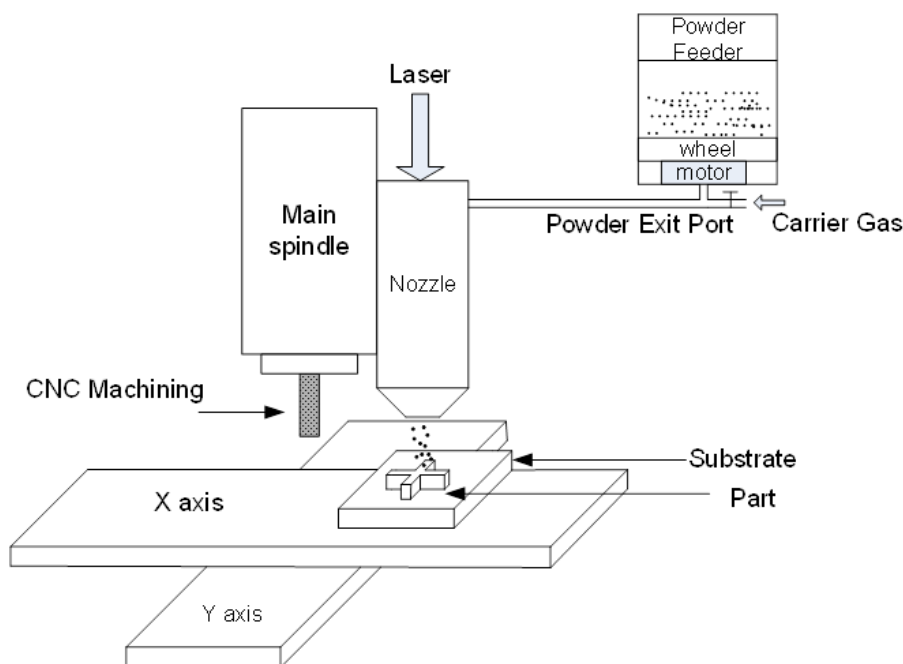
Fig. 1 Process phases for integrated material deposition and removal

For metal parts, it is difficult to find a suitable support material that can be easily separated from the building material in the post process. Also, the amount of time used in building many support structures is substantial in the overall building time. To resolve these issues, a five-axis process is proposed. The process can utilize the flexibility of the five-axis motion to greatly minimize the support structures. Due to the complexity of the part geometry, some parts cannot be built without support structures even if the process has five-axis capability. In order to keep the flexibility of the system, the building material is also used as the support material. The extra materials will be removed in a machining process. Each process needs a geometry model of the layer as shown in Fig. 2. By combining the deposition and machining processes, the resulting hybrid process provides more building capability and better accuracy and surface finish. The hybrid process can build some features that are difficult to build in the pure deposition processes.

(a) Geometry model of a layer for deposition

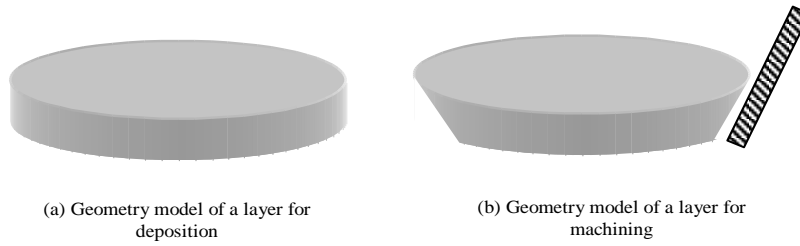(b) Geometry model of a layer for machining

Fig. 2 Geometry improvement in the deposition and machining hybrid system

The parametric representation of the tool path becomes even more important to the multi-axis hybrid process. First, the overhang deposition in a multi-axis system needs parametric representation of curves. The overhang material between two adjacent layers prevents the deposition process from building a part without support structures. After a part is sliced into layers, for each layer, it can be divided into two types of area: normal deposition area and overhang area. In traditional AM processes, the overhang needs to support structure below, which prevents the overhang material from drooping or falling. With multi-axis motion, the orientation of the nozzle can be changed which increases the possibility of building a part without support structure.

II. BACKGROUND AND TERMINOLOGIES

This section introduces some background and terminologies used in this paper. To utilize the freedom of the multi-axis motion, a method is generated for building the overhang material in a thin wall as shown in Fig. 3(a), (b). Let S_t^i be the top surface of the ith layer and S_b^i be the bottom surface, the overlap area S_n^i for layer L_i consists of the point set $\{p|p \in S_t^{i-1} \cap S_b^i \}$. The overhang area S_o^i can be expressed as

$$S_o^i = S_b^i - S_n^i. \tag{1}$$

When the overlap area is to be built, the nozzle should be oriented in the slicing direction $\vec{n}_t$, i.e., the surface normal of the top layer as shown in Fig. 3(a). When the overhang area is to be built, the nozzle should be oriented in the tangent direction of the side boundary surface of the layer, $\vec{n}_l$ as shown in Fig. 3(b). Let $C_{overlap}$ be the boundary curve of the overlap area. If the tool path is generated in offsetting $C_{overlap}$, the overhang can be built up from the side of the layer along this tool path. Because only uniform layer thickness can be achieved in the current deposition process, the distance between two offset contours is

constant. However, offsetting the linear segments of the contour directly cannot obtain the uniform offset distance as shown in Fig. 4(a). Parametric representation of curves makes the offsetting work much easier as shown in Fig. 4(b).
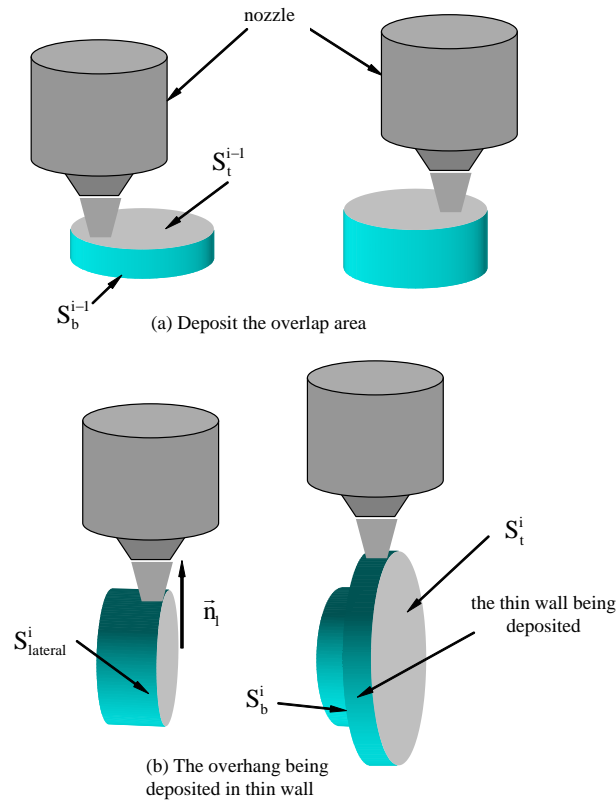

(a) Deposit the overlap area

(b) The overhang being deposited in thin wall

Fig. 3 Typical steps in thin wall deposition

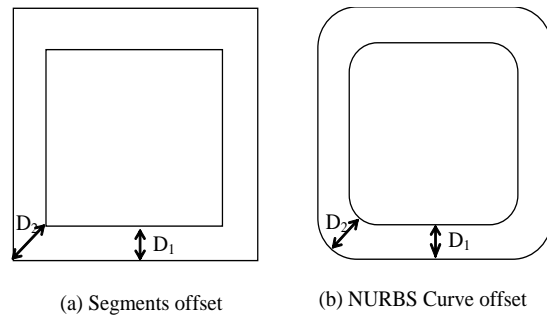(a) Segments offset   (b) NURBS Curve offset

Fig. 4 Contour offset

B-spline frequently refers to a spline curve parametrized by spline functions that are expressed as linear combinations of B-splines. The B-Spline representation of the contour is also suitable for tracking control. In the Laser Aided Manufacturing Process (LAMP) at Missouri S&T, the laser is raster scanned to fill all the layers and to build the parts layer by layer. With this type of process, there is a trade-off between productivity, in terms of build time, and part quality, in terms of surface accuracy, for a given laser power. To increase accuracy, a smaller laser spot is preferred, while productivity demands a larger laser spot to scan more area per unit time. To resolve this dilemma, Wu and Beaman [1-4] developed an optimal tracking control method for boundary scanning in Selective Laser Sintering (SLS). Chen discussed the required conditions for Wu's method in [5]. Furthermore, due to the change of building direction, the layer thickness is not uniform anymore as shown in Fig. 5(a) (b), but the slice is still planar. However, currently the laser deposition process can only build the layer with uniform thickness because it requires precise control of combination of powder feed-rate, laser power, and nozzle motion speed to achieve a non-uniform layer. The non-uniform layer is built in the following way as shown in Fig. 6(a)(b). First, the uniform layer is built in the deposition process. Then, the machining process makes the layer to the final geometry by removing the extra material. With the aid of the machining process, five-axis LAMP can produce a highly accurate part geometry and surface finish. However, most of surface machining algorithms [6-10] require that the surface be represented in parametric surface form. Currently NURBS is one of the most popular parametric surface representation forms because of its many great properties. To improve the accuracy and surface finish of the side boundary surface of a layer, the B-Spline representation is required for the machining process.
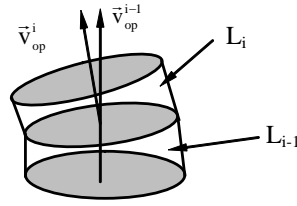
(a) Different slicing directions for two
adjacent layers respectively, $\vec{v}_{op}^{i-1}$, $\vec{v}_{op}^{i}$
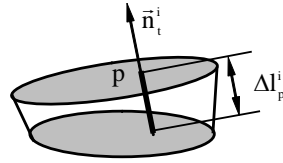
(b) Variable layer thickness

Fig. 5 Non-uniform thickness layer

(a) Deposition of uniform layer
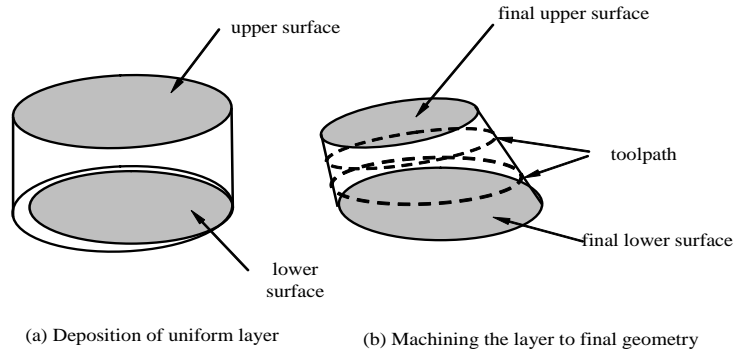
(b) Machining the layer to final geometry

Fig. 6 Two phases of non-uniform layer building

In summary, parametric spline representation is the ideal form for both deposition process and machining process. It has been adopted for the process planning of the hybrid multi-axis LAMP system.

III. NURBS CURVE FITTING FOR SLICED POINTS GENERATED FROM STL

STL (STereoLithography) is a file format native to the stereolithography CAD software created by 3D systems. STL is also a common interchange data format for Layered Manufacturing. Although several algorithms [11-13] have been developed to directly obtain the slices from the CSG (Constructive Solid Geometry) or B-Rep (Boundary-Representation) CAD model, these algorithms have some limitations. For example, Guduri et al.'s work [11] on slicing CSG representations is very complicated and slow, thus reduces the flexibility of the AM process planning. Since the slice from an STL model consists of many discrete points, a method to reconstruct the curve based on these points is needed. This problem is called curve fitting [14]. There are two types of fitting, interpolation and approximation. In interpolation, a curve which satisfies the given data precisely, i.e., the curve passes through the given points and assumes the given derivatives at the prescribed points, is constructed. Fig. 7(a) shows a curve interpolating five points and the first derivative vectors at the endpoints. In approximation, curves and surfaces which do not necessarily satisfy the given data precisely, but only approximately, are constructed. Fig. 7(b) shows a curve approximating a set of m+1 points. However, for the curve fitting of sliced points, the interpolation approach is needed.
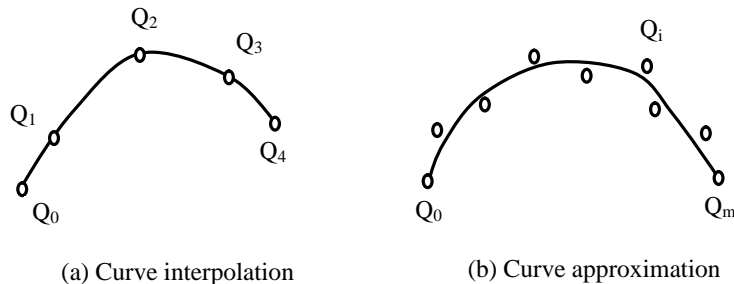

(a) Curve interpolation

(b) Curve approximation

Fig. 7 Two types of curve interpolation

A. Curve Interpolation

Interpolation is a method of constructing new data points within the range of a discrete set of known data points. Most fitting algorithms fall into one of two categories: global or local. With a global algorithm, a system of equations or an optimization problem is set up and solved. The global algorithm is sensitive to perturbation in data items. Local algorithms are more geometric in nature, constructing the curve or surface segment-wise, using only local data for each step. A perturbation in a data item only changes the curve or surface locally. Usually these algorithms are computationally less expensive than global methods. They can also deal with cusps, straight-line segments, and other local data anomalies better. Therefore, the local interpolation algorithms are used in our curve fitting.

After slicing the STL model, $\{Q_k\}$, $k = 0,\ldots,n$, for contour are given. Local curve interpolation is adapted. Local curve interpolation is a method which constructs n polynomial or rational curve segments, $\{C_i(u)\}$, $i = 0,\ldots,n-1$, such that Q_i and Q_{i+1} are the endpoints of $C_i(u)$, and the neighboring segments are joined with prescribed continuity. In the framework of NURBS, polynomial or rational Bézier curves are used to construct the segments, then obtain a NURBS curve by selecting a suitable knot vector. Cubics easily handle three-dimensional data and inflection points without special treatment. Therefore, cubic Bézier curves are used to join the segments.

Obtaining the Bézier segments, $C_i(u)$, requires computation of the inner Bézier control points, two points for cubics. These control points lie on the lines which are tangent to the curve at the Q_k; thus, tangent vectors T_k at each Q_k need to be computed. Since the sliced points from the STL model do not have the T_k information, they must be computed as part of the fitting algorithm. A number of methods exist; Boehm et al [15] gives a survey of various methods. Let

$$q_k = Q_k - Q_{k-1} \tag{2}$$

$$T_k = \frac{V_k}{|V_k|} \qquad V_k = (1-\alpha_k)q_k + \alpha_k q_{k+1} \tag{3}$$

where α_k is a coefficient representing the weight of q_k and q_{k+1} on the vector V_k. Based on a five-point method to obtain T_k [16-18], α_k is given by

$$\alpha_k = \frac{|q_{k-1} \times q_k|}{|q_{k-1} \times q_k| + |q_{k+1} \times q_{k+2}|} \qquad k = 2,\ldots,n-2 \tag{4}$$

It has the advantage that three collinear points, Q_{k-1}, Q_k, Q_{k+1}, yield a T_k which is parallel to the line segment. The denominator of Eq. (4) vanishes if Q_{k-2}, Q_{k-1}, Q_k are linear and Q_k, Q_{k+1}, Q_{k+2} are collinear. This implies either a corner at Q_k or a straight line segment from Q_{k-2} to Q_{k+2}. Although in these cases α_k can be defined in a number of ways; the definition below is chosen,

- $\alpha_k=1$, which implies $V_k=q_{k+1}$; this produces a corner at Q_k if one is implied by the data
- $\alpha_k=1/2$, which implies $V_k=1/2(q_k+q_{k+1})$; this smoothes out a corner at Q_k if one is implied by the data

Let P_0 and P_3 be two endpoints for a cubic curve segment, and T_0 and T_3 be the corresponding tangent directions with unit length. It is possible to construct a cubic Bézier curve, $C(u)$, $u \in [0,1]$, with these endpoints and tangent, to satisfy

$$\alpha = |C'(0)| = \left|C'(\frac{1}{2})\right| + |C'(1)| \tag{5}$$

where C' is the first derive of the curve $C(u)$.

The end derivatives of a Bézier curve can be obtained from

$$C'(0) = n(Q_1 - Q_0) \qquad C'(1) = n(Q_n - Q_{n-1}) \tag{6}$$

where n is the number of the points used for interpolation.

Eqs. (5) and (6) imply that

$$P_1 = P_0 + \frac{1}{3}\alpha T_0 \qquad P_2 = P_3 - \frac{1}{3}\alpha T_3 \tag{7}$$

For each Bézier curve segment, $C_k(u)$, between each pair, Q_k, Q_{k+1}, being the first and last points, denote the Bézier control points by

$$P_{k,0} = Q_k, P_{k,1}, P_{k,2}, P_{k,3} = Q_{k+1} \qquad (8)$$

Suitable locations must be determined for $P_{k,1}$ and $P_{k,2}$ along T_k and T_{k+1}, respectively. It is possible to obtain a C^l continuous cubic and achieve a good approximation to a uniform parameterization. The method is due to Renner [17]. True uniform parameterization means constant speed over the entire parameter range. A curve with equal speed at each Q_k and at the midpoint of each Bézier segment is constructed. Set $\bar{u}_0 = 0$. The two control points and $\bar{u}_{k+1}$ are computed as follows:

- Use Eq. (4) to compute α and Eq. (7) to compute $P_{k,1}$ and $P_{k,2}$;
- Set

$$\bar{u}_{k+1} = \bar{u}_k + 3|P_{k,1} - P_{k,0}| \qquad (9)$$

This algorithm yields n Bézier segments, each having speed equal to 1 at their end and midpoints with respect to their parameter ranges, $[\bar{u}_k, \bar{u}_{k+1}]$. Thus, a C^l continuous cubic B-Spline curve interpolating the Q_k is defined by the control points

$$Q_0, P_{0,1}, P_{0,2}, P_{1,1}, P_{1,2}, \ldots, P_{n-2,2}, P_{n-1,1}, P_{n-1,2}, Q_n \qquad (10)$$

and the knots

$$U = \left\{ 0,0,0,0, \frac{\bar{u}_1}{\bar{u}_n}, \frac{\bar{u}_1}{\bar{u}_n}, \frac{\bar{u}_2}{\bar{u}_n}, \frac{\bar{u}_2}{\bar{u}_n}, \ldots, \frac{\bar{u}_{n-1}}{\bar{u}_n}, \frac{\bar{u}_{n-1}}{\bar{u}_n}, 1,1,1,1 \right\} \qquad (11)$$

B. Interpolation for Accuracy Improvement

After the STL model is sliced, the point set $\{Q_k\}$, $k = 0, \ldots, n$, for contour is given. Because the curve passes through all the given points and assumes the given derivatives at the prescribed points, the density of the given points increases the interpolation accuracy. Therefore, if an algorithm can increase the density of the given points, the desired interpolation accuracy can be achieved. The density of the given points can be represented by the maximum distance between two adjacent points, Q_k and Q_{k+1}. Let D be the maximum distance between Q_k and Q_{k+1}. In general, it is very difficult to increase the density of the input points to any desired small value ε. Fortunately, the STL model has a property to make the point density increase possible. As discussed previously, the STL model consists of many triangles. After the STL model is cut by the slicing plane, the contour that consists of several segments is obtained. These segments are on the boundary surface of the part. Therefore, an interpolation is conducted between any two adjacent points, Q_k and Q_{k+1} between which the distance is larger than ε. The interpolation adds n new points to the point set. n is given

$$n = floor(\frac{D}{\varepsilon}) + 1 \qquad (12)$$

where $floor(x)$ is defined as the maximum integer that satisfies $floor(x) \le x$. The n new points are given by,

$$Q_k^i = Q_k + \frac{i}{n}(Q_{k+1} - Q_k) \qquad i = 1, \ldots, n \qquad (13)$$

IV. RULED SIDE SURFACE CONSTRUCTION FOR LAYERS

A multi-axis adaptive slicing algorithm has been applied in multi-axis LAMP system [19]. This adaptive slicing not only adaptively varies the layer thickness but also the slicing direction. As shown in Fig. 8 the cusp height C represents the slicing error and is given by,

$$S_{error} = \frac{C^2}{2\sin\theta\cos\theta} \qquad (14)$$

where θ is the angle between the surface normal and the building direction, C is the cusp height.
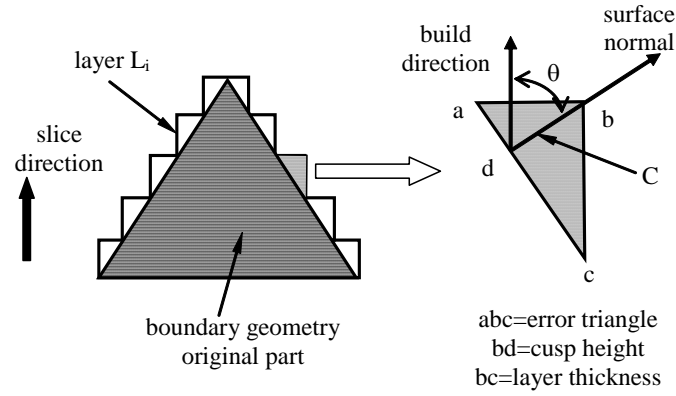
Fig. 8 Error triangle between sliced layers and original part geometry

Therefore, the maximum allowed cusp height C_{max} in the slicing determines the accuracy of the slicing result. After the contour of the slice is obtained, the zero or first order approximation can be applied to construct the side surface of two adjacent slices. The difference between these two approximations affects how accurate the layers approximate the original geometry. Substantial research work has been carried out in the area of first order approximation of model geometry. The term, *twisted profile layers,* is used in [20] to describe ruled slices. Layers with sloping side surfaces are also used in [21] for the manufacturing of large objects. In geometry, a surface S is ruled (also called a scroll) if through every point of S there is a straight line that lies on S. Ruled layers are also used for the CAM-LEM process [22] and the Shapemaker II process [23]. The difference between the 2.5-D slices and the ruled slices is shown schematically in Fig. 9. The processes that can produce ruled slices have at least four degrees of freedom (translation in the x, y plane and additional rotations φ, θ). These processes could be CNC milling, laser cutting and more.
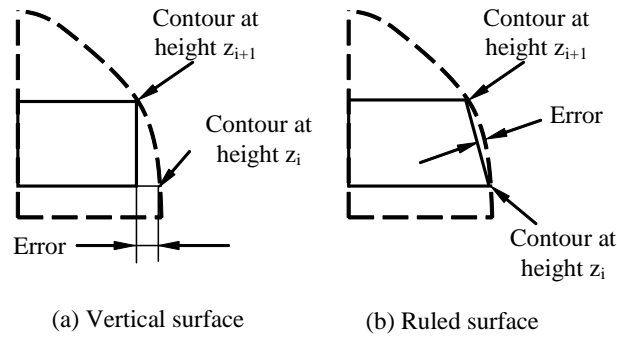

(a) Vertical surface   (b) Ruled surface

Fig. 9 Difference between zero order and first order approximation

A horizontal layer (in the x, y plane) with a vertical outer surface can be regarded as a zero order approximation in the vertical slicing direction (z) of a part of the original model geometry. The usual procedure to reconstruct such a layer is to slice the model and to extrude the slice into the slicing direction to give the slice a certain thickness. In general, this will result in an error everywhere around the contour. This error depends on the local curvature and the inclination relative to the slicing direction. Let P be a point on the surface, θ is the angle that the surface normal makes to the horizontal, ρ is the radius of curvature at P, δ is the allowed cusp height and d is the thickness of the layer. The formula for circular approximation depends on whether positive/negative tolerance is desired, if the curvature is positive/negative, and also if the point P lies in the upper/lower semicircle of the circle of curvature. The formula is derived into two categories [24]

- Negative Tolerance

$$d = \mp \rho \sin \theta \pm \sqrt{\rho^2 \sin^2 \theta \pm 2\rho\delta \mp \delta^2} \tag{15}$$

P in upper semicircle, (the sign depends on $\kappa > 0$ or $\kappa < 0$)

$$d = \mp \rho \sin \theta \pm \sqrt{\rho^2 \sin^2 \theta \pm 2\rho\delta \pm \delta^2} \tag{16}$$

P in lower semicircle, (the sign depends on $\kappa > 0$ or $\kappa < 0$)

- Positive Tolerance

$$d = \mp \rho \sin \theta \pm \sqrt{\rho^2 \sin^2 \theta \pm 2\rho\delta \pm \delta^2} \tag{17}$$

P in upper semicircle, (the sign depends on $\kappa > 0$ or $\kappa < 0$)

$$d = \mp \rho \sin \theta \pm \sqrt{\rho^2 \sin^2 \theta \pm 2\rho\delta \mp \delta^2} \qquad (18)$$

P in lower semicircle, (the sign depends on $\kappa > 0$ or $\kappa < 0$)

The first order approximation is based on constructing the ruled surface between successive contours using geometrical and topological information from the original geometry. A ruled surface is generated by a family of straight lines. An expression based on joining corresponding points on two space curves $r = r_0(u)$ and $r = r_1(u)$ is given by

$$r = r(u,v) = (1-v)r_0(u) + vr_1(u) \qquad (19)$$

The curves $r = r_0(u)$ and $r = r_1(u)$ are known as directrices, and the rulings are called generators. An advantage of ruled slicing is that, because the edges of the adjacent slices meet, C^0 continuity in the slicing direction is guaranteed, eliminating the staircase effect as present in the 2.5-D approach. An improved surface finish is the result. Another advantage is the reduction in the number of layers. For ruled slicing an expression for the error and thus for the allowed layer thickness can be derived as [25]

$$d = \cos\theta\sqrt{2\rho\delta - \delta^2} \qquad (20)$$

V. BRANCHING AND MATCHING PROBLEM IN CONSTRUCTION OF RULED SURFACE

To form a ruled surface, two successive contours that are connected by the surface must be found. This is difficult because of the branching and the correspondence problem as shown in Fig. 10. In the branching problem the number of contours is different between two successive slices. In the correspondence problem the number of contours per slice is the same but larger than one for two successive slices, and it is unknown which pair of contours should be connected from one slice to the other.
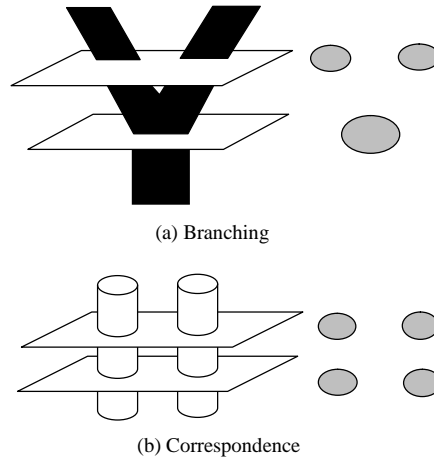

(a) Branching

(b) Correspondence

Fig. 10 Branching and correspondence

(a) Surface construction in
diverging case
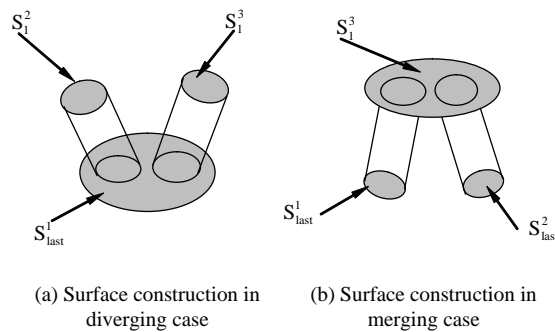
(b) Surface construction in
merging case

Fig. 11 Side surface construction for diverging case and merging case

The branches can be identified when the multi-axis adaptive slicing algorithm is applied [19]. However, it is necessary to find a reasonable method to construct the surface at the branching point. There are two cases in branching: diverging and merging. As shown in Fig. 11(a), in the diverging case the surface for the joint is generated in sweeping the slice S_1^2 in the branch 2 along the negative normal direction until it reaches the last slice S_{last}^1 in the branch 1. As shown in Fig. 11(b), in the

merging case, the surface for the joint is generated in sweeping the slice S^1_{last} in the branch 2 along the positive normal direction until it reaches the last slice S^3_1 in the branch 1. However, if the sweeping of the two slices intersect, the wrong surface will be constructed. In this case, a new slice in the parent branch that the other branches diverge from or merge to is generated between the slices in child branches and the slice in the parent branch is shown in Fig. 12 so that no intersection will occur.

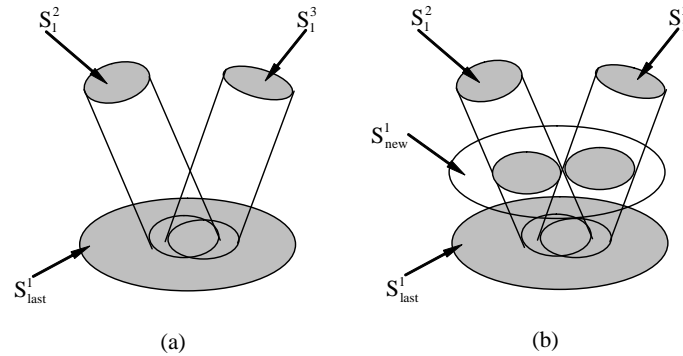(a)   (b)

Fig. 12 Interpolation between slices in different branches

The matching can be accomplished using either matching in parameter space [25] or matching in geometric space so that the correct starting points on the successive contours can be found. The method in [26] cannot be used for the STL model because it is based on B-Rep surface topology information. A method based on facets topology information, which is similar to the contour matching algorithm in [27] is developed. The matching algorithm has two steps: direct adjacent test, indirect adjacent test.

A. Direct Adjacency Test

In the direct test, each segment of the contour on the lower slice is searched for any facet that is also a member of a contour on the above adjacent slice. If such a facet exists, then the two segments in question are best matching. A pair of two adjacent endpoints among these four can be used as the start points respectively for $r_0(u)$ and $r_1(u)$ in Eq. (18) to form the ruled surface as shown in Fig. 13.
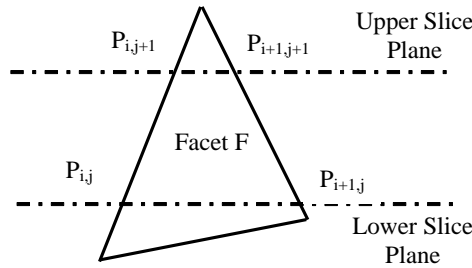

Fig. 13 Direct adjacency test

B. Indirect Adjacency Test

In cases where the direct adjacent test fails, a computationally more expensive indirect test is applied. A steepest gradient climb upward from each of the facets on the lower contours is performed in attempt to reach the upper contours as shown in Fig. 14. Once a segment on the upper contour is found, the start points can be determined similarly to the method used for the direct adjacency test.
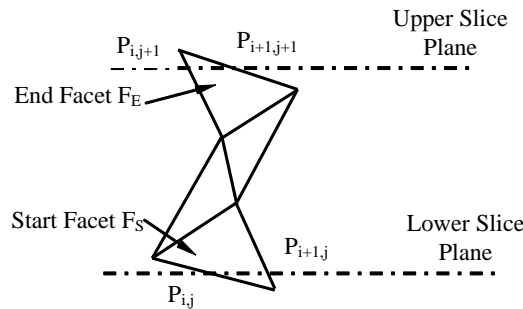

Fig. 14 Indirect adjacency test

As the follow up work, the multi-axis slicing approach studied utilizes the skeleton-like shape to guide the slicing procedure [28-30]. This slicing procedure uses either a 3-D layer or a parallel layer, as needed. Following the slicing results, the deposition process fabricates a shape which is closer to the desired geometry. As the 3-D layer is a critical issue in multi-axis slicing processes, directly fabricating 3-D layers plays an important role in advancing multi-axis laser metal deposition processes. An automated machining process planning has also been researched and implemented [31].

VI. EXAMPLES

In Fig. 15 and Fig. 16, the reconstructed approximation models from slicing and interpolation from two modelsare shown. In the examples only side surfaces have been constructed. This is because the top and bottom surfaces of the layer are planar and the machining process for this surface is simple. Table 1 shows the part dimension and slicing parameters of the two examples. In Fig. 15 a rendering of the result for a simple shape is shown in comparison between the original model and the approximation result.
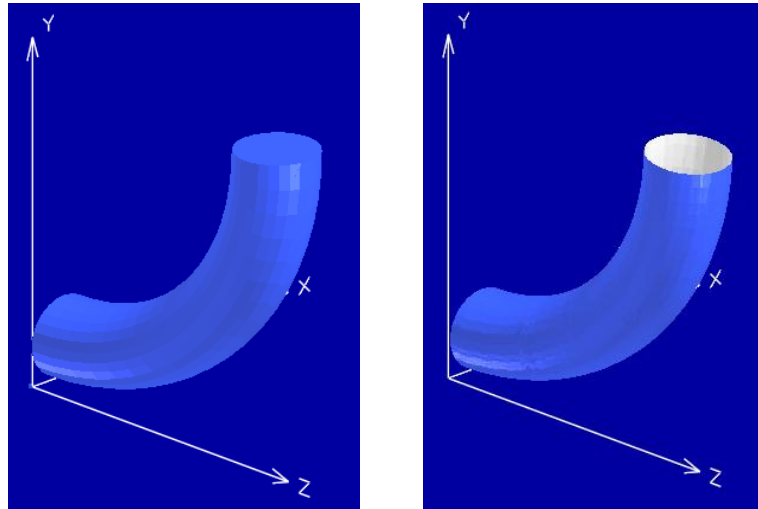

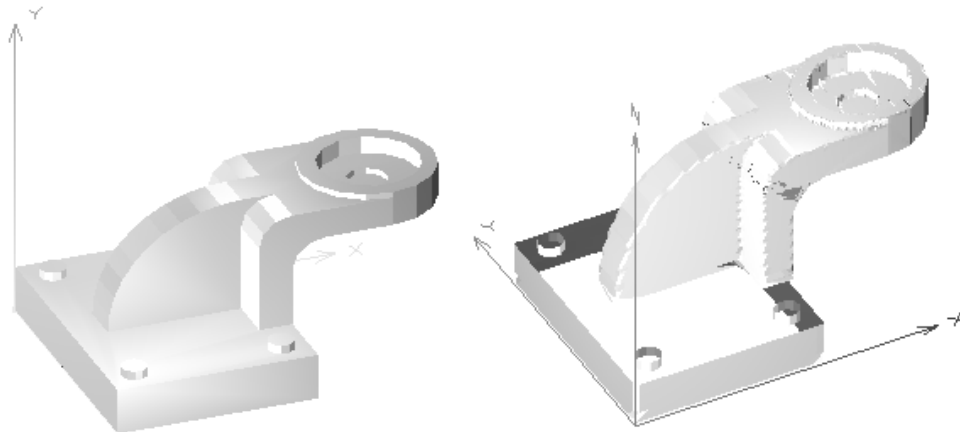Fig. 15 A pipe (left) and the approximation

Fig. 16 A bearing and the approximation (right)

TABLE 1 PART DIMENSION AND SLICING PARAMETERS OF THE TWO EXAMPLES

	Boundary Box Dimension	Maximum Allowable Cusp Height C_{max}
Example1	L=11mm, W=46mm, H=46mm	0.04mm
Example2	L=55mm, W=29mm, H=40mm	0.08mm

In Fig. 16 the results for a more complex geometry are shown. This part consists of straight walls, a blind hole and four small cylinders. It can be easily seen that the branching and the correspondence between the adjacent contours are solved correctly.

Fig. 17 shows the slicing result of a double-arc example, which demonstrates the usage of "3-D" layers. The slicing direction is kept changed to reflect the direction change in the centroidal axis. This matches the geometry shape in two curved branches.

(a) Decomposition result   (b) Slicing result
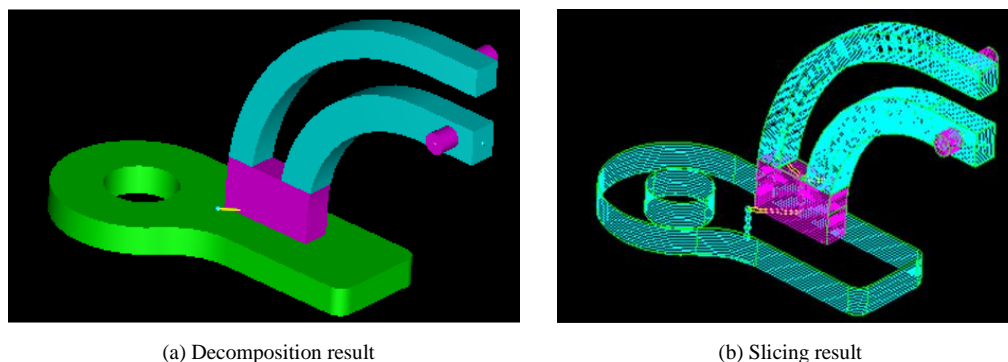
Fig. 17 Slicing result of the double-arc example

A hinge example and its deposition result are shown in Figure 18. The part is decomposed into five subcomponents (1, 2, 3, 4, 5) as shown in Figure 18(c). The slicing result is shown in Figure 18(d). The deposition starts from building the subcomponent 1 then the subcomponents 2, 3 are built after rotating the part 90° around X axis. The subcomponents 4, 5 are finished after rotating the part 180° around Y axis.
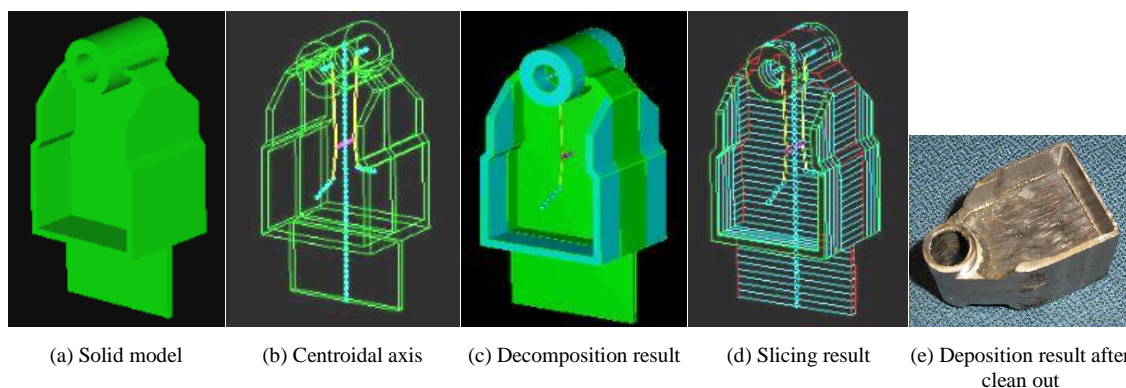

(a) Solid model   (b) Centroidal axis   (c) Decomposition result   (d) Slicing result   (e) Deposition result after clean out

Fig. 18 Hinge example

VII.   CONCLUSIONS

The parametric representation of a curve as presented in this paper is very important to the automatic path planning process for the hybrid material deposition and removal without support structure. Successful utilization of different geometric representations by AM technologies requires the development of algorithms to extract and convert the geometric information correctly. NURBS can be used to represent these geometric features after they are recognized. The algorithms presented in this paper can reconstruct the parametric curve for layer contour and parametric surface for machining process to the desired accuracy by interpolating more points between given points. The accuracy of the model will be dependent on the accuracy of the STL file and the level of continuity as discussed in this paper. In general, the higher the accuracy, the larger the STL file size.

REFERENCES

[1] Wu, Y-J.E., and Beaman, J.J., "Solid Freeform Fabrication Laser Tracking Control", *Solid Freeform Fabrication Proceedings*, Austin, TX, pp. 37-45, 1991.

[2] Wu, Y-J.E., and Beaman, J.J., "Contour Following for Scanning Control in SFF Application: Control Trajectory Planning", *Solid Freeform Fabrication Proceedings*, Austin, TX, pp. 126-134, 1990.

[3] Wu, Y-J.E., and Beaman, J.J., "Laser Tracking Control Implementation for SFF Applications", *Solid Freeform Fabrication Proceedings*, Austin, TX, pp. 161-173, 1992.

[4] Wu, Y-J.E., 1992, "A Minimum Time Laser Tracking Control Technique For Selective Laser Sintering", *Ph.D. Thesis*, The University of Texas at Austin, Austin, TX.

[5] Chen, K., Crawford, R. H., and Beaman, J. J., "Parametric Representation of Part Contours in SLS Process", *Solid Freeform Fabrication Proceedings*, Austin, TX, pp. 597-608, 1996.

[6] Lee, Y.S., "Non-isoparametric Tool Path Planning by Machining Strip Evaluation for 5-axis Sculptured Surface Machining", *Computer-Aided Design*, vol. 30, iss. 7, pp. 559-570, 1998.

[7] Hwang, J.S., "Interference-free Tool-path Generation in the NC Machining of Parametric Compound Surfaces", *Computer Aided Design*, vol. 24, iss. 12, pp. 667-679, 1992.

[8] Suh, Y.S. and Lee, K., "NC Milling Tool Path Generation for Arbitrary Pockets Defined by Sculptured Surfaces", *Computer-Aided Design*, vol. 22, iss. 5, pp. 273-284, 1990.

[9] Suh, S.H. and Lee, J.J., "Five-axis Part Machining With Three-Axis CNC Machine and Indexing Table", *Journal of Manufacturing Science & Engineering, Transactions of the ASME*, vol. 120, iss. 1, pp. 120-128, 1998.

[10] Elber, G. and Fish R., "Five-Axis Freeform Surface Milling Using Piecewise Ruled Surface Approximation", *Journal of Manufacturing Science and Engineering*, vol. 119, pp. 383-387, 1997.

[11] Guduri, S., Crawford, R. H., and Beaman, J. J., "Direct Generation of Contour Files from Constructive Solid Geometry Representations", *Solid Freeform Fabrication Proceedings*, Austin, TX, pp. 291-302, 1993.

[12] Vuyyuru, P., Kirschman, C., Fadel, G., and Bagchi, A., "A NURBS-Based Approach for Rapid Prototyping Realization", *International Conference on Rapid Prototyping*, Dayton, OH, pp. 229-240, 1994.

[13] Rajagopalan, M., Aziz, N.M., and Huey, Jr. C.O., "A model for interfacing geometric modeling data with rapid prototyping systems", *Proceedings of the Fifth International Conference on Rapid Prototyping*, Dayton, OH, pp. 229-239, 1994.

[14] Piegl, L. and Tiller, W., 1997, *The NURBS Book*, second Edition, Springer.

[15] Boehm, W., Farin, G., and Kahmann, J., "A Survey of Curve and Surface Methods in CAGD", *Computer Aided Geometric Design*, vol. 1, iss. 1, pp. 1-60, 1984.

[16] Akima, H., "A new method of interpolation and smooth curve fitting based on local procedures", *Journal of ACM*, vol. 17, pp. 589-602, 1970.

[17] Renner, G., "A Method of Shape Description for Mechanical Engineering Practice", *Computer In Industry*, vol. 3, pp. 137-142, 1982.

[18] Pergl, L., "Interactive Data Interpolation by Rational Bézier Curves", *IEEE Computer Graphics And Application*, vol. 7, iss. 4, pp. 45-58, 1987.

[19] Zhang, J. and Liou, F.W., 2001, "Adaptive Slicing for a Five-axis Laser Aided Manufacturing Process", *Proceedings of ASME DAC Conference*, Pittsburgh, Pennsylvania.

[20] Barlier, C., Gasser, D., Muller, F. and Feltes, U., "Stratoconception-Rapid Prototyping for Die-forging Tooling", *Proceedings of the 28th ISATA Conference*, Dedicated on Rapid Prototyping in the Automotive Industries, Stuttgart, Germany, pp. 61-67, 1995.

[21] Hope, R.L., Riek, A.T. and Roth, R.N., "Layer Building with Sloped Edges for Rapid Prototyping of Large Objects", *Proceedings of the 5th European Conference on Rapid Prototyping and Manufacturing*, Helsinki, pp. 47-58, 1996.

[22] Newman, M., Zheng, Y. and Fong, C.C., "Trajectory Generation from CAD Models for Computer-aided Manufacturing of Laminated Engineering Materials", *Proceedings of the 26th International Symposium on Industrial Robots*, Singapore, pp. 153-158, 1995.

[23] Thomas, C.L., Gaffney, T.M., Kaza, S. and Lee, C.H., "Rapid Prototyping of Large Scale Aerospace Structures", *Proceedings of the 1996 IEEE Aerospace Applications Conference*, vol. 4, pp. 219-230, 1996.

[24] Kulkarni, P. and Dutta, D., "An Accurate Slicing Procedure for Layered Manufacturing", *Computer Aided Design*, vol. 28, iss. 9, pp. 683-697, 1996.

[25] Jager, de P.J., "Using Slanted and Ruled Layers for Rapid Prototyping", *Proceedings of the 5th European Conference on Rapid Prototyping and Manufacturing, Helsinki*, pp. 15-30, 1996.

[26] Jager, de P.J., Broek, J.J., and Vergeest, J.S.M., "A Comparison between Zero and First Order Approximation Algorithms for Layered Manufacturing", *Assembly Automation*, vol. 3, iss. 4, pp. 233-238, 1997.

[27] Tyberg, J. and Bohn, J.H., "Local Adaptive Slicing", *Rapid Prototyping Journal*, vol. 4, iss. 3, pp. 118-127, 1998.

[28] Ruan, J., Sparks, T., Panackal, A., Liou, F.W., Eiamsa-ard, K., Slatter, K., Chou, H., and Kinsella, M., "Automated Slicing for a Multiaxis Metal Deposition System", ASME Journal of Manufacturing Science and Engineering, vol. 129, pp 303-310, 2007.

[29] Ren, Lan, Todd Sparks, Jianzhong Ruan, and Frank Liou, "Integrated Process Planning Framework for a Multi-axis Hybrid Manufacturing System," ASME Journal of Manufacturing Science and Engineering, vol. 132/021006-1 to 021006-7, April 2010.

[30] Ruan, Jianzhong, Lie Tang, Todd E. Sparks, Frank Liou, and Robert G. Landers, "Direct Three Dimensional Layer Metal Deposition," ASME Journal of Manufacturing Science and Engineering, vol.132, iss. 6, pp. 064502-1 to 064502-6, 2010.

[31] Francis, Jomy, Todd Sparks, and Frank Liou, "Uncertainty Analysis in Laser Deposition Finish Machining Operations," Proceedings of the 21st Solid Freeform Fabrication Symposium, Austin, Texas, August 9-11, 2010.

[32] Zhang, Jun and F.W. Liou, "Adaptive Slicing for A Multi-axis Laser Aided Manufacturing Process," ASME Journal of Mechanical Design, vol. 126, pp. 254-261, March 2004.

[33] Ruan, J., K. Eiamsa-ard, and F. Liou, "Automatic Process Planning and Toolpath Generation of a Multi-Axis Hybrid Manufacturing System," SME Journal of Manufacturing Processes, vol. 7, iss. 1, pp. 57-68, 2005.